Magic angle spinning oxygen-17 NMR of aluminum oxides and hydroxides

ARTICLE *in* THE JOURNAL OF PHYSICAL CHEMISTRY · SEPTEMBER 1989

Impact Factor: 2.78 · DOI: 10.1021/j100355a034

2 AUTHORS, INCLUDING:

Thomas H Walter
Waters Corporation
25 PUBLICATIONS **1,021** CITATIONS

SEE PROFILE

Magic Angle Spinning Oxygen-17 NMR of Aluminum Oxides and Hydroxides†

Thomas H. Walter‡ and Eric Oldfield*

School of Chemical Sciences, University of Illinois at Urbana-Champaign, Urbana, Illinois 61801
(Received: December 5, 1988; In Final Form: April 24, 1989)

We have obtained magic angle spinning ^{17}O nuclear magnetic resonance spectra of ^{17}O-labeled α-Al_2O_3, boehmite (AlO(OH)), bayerite ($Al(OH)_3$), and several transitional aluminas, including γ-, η-, δ-, and θ-Al_2O_3. Cross polarization from ^1H to ^{17}O has been used to enhance the hydroxyl oxygen resonances of boehmite and bayerite and to allow the observation of hydroxyl groups on the surface of γ-Al_2O_3. The spectra yield nuclear quadrupole coupling constants, electric field gradient tensor asymmetry parameters, and isotropic chemical shifts for each chemically distinct oxygen site. The quadrupole coupling constants for tetrahedrally coordinated oxide sites (OAl_4) range from 1.2 to 2.2 MHz, while those of trigonally coordinated hydroxide sites (Al_2OH) are in the 5-6-MHz range. Trigonally coordinated oxide sites (OAl_3), arising as a result of cation vacancies in the transitional aluminas, are estimated to have quadrupole coupling constants of approximately 4 MHz. It is shown that the observed quadrupole coupling constants and asymmetry parameters are in generally good agreement with the results of electric field gradient calculations based on a point charge model.

Transitional aluminas, intermediate dehydration products of aluminum hydroxides and oxide hydroxides, are among the most widely used catalysts and catalyst supports.[1,2] Although alumina itself catalyzes a variety of carbonium ion mediated hydrocarbon isomerization and cracking reactions, it is most commonly employed as a support for noble metal crystallites in petroleum reforming catalysts.[3] Transitional aluminas are also an important component of supported molybdena catalysts, which are used for hydrodesulfurization of high-sulfur petroleum feedstocks.[4] While over a dozen distinct alumina phases have been described, the γ and η forms, derived from boehmite and bayerite, respectively, are the most important in catalysis.[2] As indicated by the dehydration sequences shown below, dehydration of boehmite (an AlO(OH) polymorph) and bayerite (an $Al(OH)_3$ polymorph) proceeds through a series of alumina phases having distinct X-ray diffraction patterns, which are known collectively as transitional, or active, aluminas:[1]

$$\text{boehmite (crystalline)} \xrightarrow{450\ ^\circ C} \gamma\text{-}Al_2O_3 \xrightarrow{600\ ^\circ C} \delta\text{-}Al_2O_3 \xrightarrow{1200\ ^\circ C} \alpha\text{-}Al_2O_3$$

$$\text{bayerite} \xrightarrow{230\ ^\circ C} \eta\text{-}Al_2O_3 \xrightarrow{850\ ^\circ C} \theta\text{-}Al_2O_3 \xrightarrow{1200\ ^\circ C} \alpha\text{-}Al_2O_3$$

Upon dehydration at 1200 °C, all aluminum hydroxides and oxides are converted to α-Al_2O_3, which has the well-known corundum structure.[5] In contrast, the transitional aluminas have highly disordered microporous strucures, and high surface areas. One important feature of the transitional aluminas is the presence of hydroxyl groups at exposed crystallite faces.[6] Since the catalytic properties of aluminas predominantly reflect their surface, rather than bulk structure, these surface hydroxyl groups play a key role in the catalytic reactions of aluminas.

The ^{27}Al NMR spectra of several transitional aluminas have been described,[7,8] and it has been shown that magic angle spinning (MAS) ^{27}Al NMR can be used to distinguish between aluminum in tetrahedral and octahedral coordination. Oxygen, the other framework element of alumina, is considerably less attractive from an NMR standpoint, since the only magnetically active nuclide, ^{17}O ($I = 5/2$), has both low natural abundance (0.037%) and a low gyromagnetic ratio. However, as recently demonstrated,[9-13] the use of isotopically enriched materials in conjunction with high magnetic fields enables the observation of solid-state ^{17}O NMR spectra, providing new information on structure and bonding in a variety of inorganic solids, including minerals,[9,11] glasses,[12] and zeolites.[13] In this article, we describe an ^{17}O NMR investigation of a variety of ^{17}O-enriched aluminum hydroxides and oxides. The results for several well-defined phases, α-Al_2O_3, AlO(OH), and $Al(OH)_3$, are used to interpret the spectra of the more ill-defined transitional aluminas.

Experimental Section

Chemical Aspects. Samples were enriched to ca. 20-50% in ^{17}O either by direct synthesis or by exchange with $H_2{}^{17}O$ (Cambridge Isotopes, Woburn, MA). Oxygen-17 enriched gelatinous boehmite was prepared by exchange between $H_2{}^{17}O$ and gelatinous boehmite (CATAPAL SB, Conoco Chemicals, Houston, TX) at 105 °C for 24 h. Oxygen-17 enriched crystalline boehmite was prepared from gelatinous boehmite and $H_2{}^{17}O$ in sealed gold tubes under hydrothermal conditions (400 °C, 1000 psi, 4 days) in a stainless steel pressure vessel. Oxygen-17 enriched bayerite was prepared by hydrolysis of amalgamated aluminum with $H_2{}^{17}O$, following the procedure of Schmah.[14] Although this sample appeared pure by X-ray powder diffraction, ^{17}O NMR reveals that it contains a significant amount (ca. 10%) of gelatinous boehmite (vide infra). Enriched aluminum oxides were prepared by dehydration of [^{17}O]-boehmite and [^{17}O]-bayerite under an air atmosphere in a muffle furnace. All samples were dried at 120 °C for 24 h to remove adsorbed $H_2{}^{17}O$ and were stored in a desiccator to minimize adsorption of atmospheric moisture. The purity of each sample was verified by powder x-ray diffraction.

Nuclear Magnetic Resonance Spectroscopy. Oxygen-17 NMR spectra were obtained on FT-NMR spectrometers operating at 67.8 and 48.8 MHz, which have previously been described.[13,15]

† Taken in part from the Ph.D. Thesis of T. H. Walter, University of Illinois at Urbana-Champaign, 1987.

‡ Present address: Millipore, Waters Chromatography Division, 34 Maple St., Milford, MA 01757.

(1) Lippens, B. C.; Steggerda, J. J. In *Physical and Chemical Aspects of Adsorbents and Catalysts*; Linsen, B. G., Ed.; Academic: London, 1970; p 171.
(2) Oberlander, R. K. In *Applied Industrial Catalysis*; Leach, B. E., Ed.; Academic: Orlando, FL, 1984; Vol. 3, p 63.
(3) Sinfelt, J. H. In *Catalysis Science and Technology*; Anderson, J. R., Boudart, M., Eds; Springer-Verlag: Berlin, 1981; p 257.
(4) Schuit, G. C. A.; Gates, B. C. *AIChE J.* **1973**, *19*, 417.
(5) Ishizawa, N.; Miyata, T.; Minato, I.; Marumo, F.; Iwai, S. *Acta Crystallogr.* **1980**, *B36*, 228.
(6) Knozinger, H.; Ratnasamy, P. *Catal. Rev. Sci. Eng.* **1978**, *17*, 31.
(7) Mastikhin, V. M.; Krivoruchko, O. P.; Zolotovskii, B. P.; Buyanov, R. A. *React. Kinet. Catal. Lett.* **1981**, *18*, 117.
(8) John, C. S.; Alma, N. C. M.; Hays, G. R. *Appl. Catal.* **1983**, *6*, 341.
(9) Schramm, S.; Oldfield, E. *J. Am. Chem. Soc.* **1984**, *106*, 2502.
(10) Janes, N.; Oldfield, E. *J. Am. Chem. Soc.* **1986**, *108*, 5743.
(11) Timken, H. K. C.; Schramm, S. E.; Kirkpatrick, R. J.; Oldfield, E. *J. Phys. Chem.* **1987**, *91*, 1054.
(12) Bray, P. J. In *Borate Glasses: Structure, Properties, Applications*; Pye, L. D., Frechette, V. D., Kreidl, N. J., Eds, Plenum: New York, 1977; p 321.
(13) Timken, H. K. C.; Turner, G. L.; Gilson, J. P.; Welsh, L. B.; Oldfield, E. *J. Am. Chem. Soc.* **1986**, *108*, 7231.
(14) Schmah, V. H. *Z. Naturforsch* **1946**, *1*, 323.

0022-3654/89/2093-6744$01.50/0

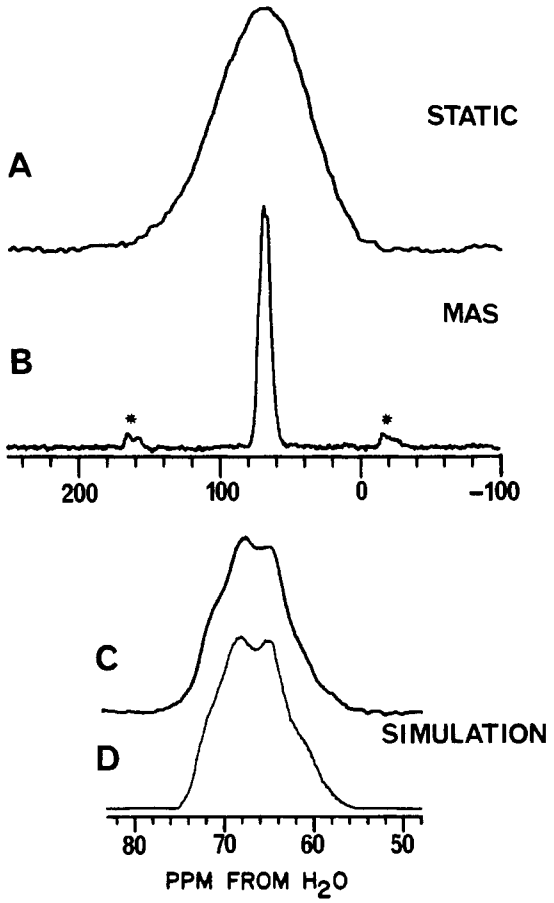

Figure 1. Oxygen-17 NMR spectra of α-Al_2O_3 obtained at 68 MHz. (A) Stationary sample; 1376 acquisitions with a 30-s recycle time. (B) MAS spectrum; 6.1 kHz spinning speed, 356 acquisitions with a 30-s recycle time (* indicates spinning sidebands). (C) Expanded view of MAS spectrum. (D) Simulated spectrum using C_Q = 2.17 MHz, η = 0.55, δ_i = 75 ppm, 65 Hz line broadening.

For experiments requiring a spectral width in excess of 125 kHz, a Nicolet (Nicolet Instrument Corp., Madison, WI) 204-A 50-ns transient recorder was used for data acquisition. Static and MAS NMR spectra at both field strengths were obtained using Doty probes (Doty Scientific, Columbia, SC). Spectra were obtained by using 90° pulse excitation, with a 5-μs pulse width (corresponding to a 15-μs 90° pulse width for the H_2O reference). Cross-polarization spectra were obtained as previously described,[15] using ^{17}O and ^1H radio frequency field strengths of 16.7 and 50 kHz, respectively. Chemical shifts are reported in parts per million (ppm) from an external sample of water, with the low-field (high-frequency) values being designated as positive, in accord with the IUPAC (δ scale) convention. Quadrupole coupling constants, asymmetry parameters, and chemical shifts were obtained by computer simulation of the experimental spectra. The chemical shifts derived from these simulated line shapes are the true values, corrected for the second-order quadrupolar shift.[16] The ^{17}O spin-lattice relaxation times (T_1) for these samples were found to vary over a wide range. As previously noted,[15] T_1's for the hydroxyl oxygen sites are found to be relatively short, on the order of 100 ms. However, for the OAl_4 sites of boehmite, γ-Al_2O_3 and η-Al_2O_3, we find apparent T_1's on the order of 2–10 s, measured by using the saturating comb saturation-recovery method.[17,18] For the OAl_4 resonances of α-Al_2O_3, and the high-temperature transitional aluminas (δ and θ), we find that the T_1's have increased to ca. 100 s, necessitating the use of long delays between pulses.

TABLE I: Oxygen-17 Nuclear Quadrupole Coupling Constants, Asymmetry Parameters, and Isotropic Chemical Shifts for Aluminum Oxides and Hydroxides[a]

system	site	C_Q, MHz	η	δ_i, ppm
α-Al_2O_3	OAl_4	2.17 (±0.05)	0.55 (±0.05)	75 (±2)
AlO(OH)	OAl_4	1.20 (±0.05)	0.1 (±0.1)[b]	70 (±1)
(boehmite)	Al_2OH	5.0 (±0.2)	0.5 (±0.1)	40 (±5)
$Al(OH)_3$ (bayerite)	Al_2OH	6.0 (±0.2)	0.3 (±0.1)	40 (±5)
γ-Al_2O_3	OAl_4	1.8 (±0.2)[c]		73 (±1)[c]
η-Al_2O_3	OAl_4	1.6 (±0.2)[c]		73 (±1)[c]
δ-Al_2O_3	OAl_4	1.6 (±0.2)[c]		72 (±1)[c]
θ-Al_2O_3	OAl_4	1.2 (±0.2)[c]		72 (±1)[c]
	OAl_3	4.0 (±0.2)	0.6 (±0.1)	79 (±5)

[a] All parameters derived from simulations of 67.8-MHz MAS spectra, unless otherwise noted. [b] Value obtained from simulation of spinning sideband pattern. [c] Value calculated from quadrupole shift.

Results and Discussion

α-Al_2O_3. The structure of α-Al_2O_3 (corundum) consists of a hexagonal close-packed array of oxide ions, with the aluminum ions distributed among the octahedral interstices. The structure contains a single oxygen site, with oxygen coordinated to four aluminum ions (hereafter designated OAl_4) in a site with C_2 symmetry.[5] We show in Figure 1A,B static and MAS ^{17}O NMR spectra of an ^{17}O-enriched sample of α-Al_2O_3, prepared by dehydrating gelatinous boehmite at 1200 °C for 1 h. As previouly shown,[9] the spectrum obtained without magic angle spinning is a featureless, approximately Gaussian resonance, with a width at half-height of ca. 5 kHz. This line shape arises from a second-order quadrupolar powder pattern broadened by dipolar coupling between ^{17}O and the 100% abundant ^{27}Al nuclide. Using an Al–O bond distance of 1.85 Å, we estimate an ^{17}O–^{27}Al dipolar second moment[19] of 1.2 kHz for an OAl_4 unit, which is sufficiently large to completely obscure the quadrupolar line shape. However, this dipolar broadening can be eliminated by MAS, as shown in Figure 1B, leaving a quadrupolar line shape that has been only partially averaged by spinning at the magic angle.[20] Simulation of this line shape (Figure 1D) yields a quadrupole coupling constant (C_Q) of 2.17 MHz, and an asymmetry parameter (η) of 0.55 (Table I), in excellent agreement with the values determined for a single crystal of ruby (Al_2O_3:Cr^{3+}): C_Q = 2.167 MHz, η = 0.517.[21]

AlO(OH). Aluminum oxide hydroxide occurs in two distinct forms: boehmite and diaspore, although a distinction should also be made between gelatinous boehmite (also known as pseudoboehmite), which is produced by precipitation from aqueous solutions of Al^{3+} salts, and crystalline boehmite, which is formed under hydrothermal conditions.[1] The oxide hydroxides are sheet structures, built up from edge-sharing $AlO_4(OH)_2$ or $AlO_3(OH)_3$ octahedra. While diaspore and boehmite differ in the packing arrangement between successive sheets, gelatinous and crystalline boehmite differ primarily in the degree of polymerization of the $AlO_4(OH)_2$ units.[2] As a result of the lower extent of polymerization, gelatinous boehmite characteristically contains excess water, present as terminating groups, and gives rise to broad X-ray powder diffraction lines.

The boehmite structure contains two distinct oxygen sites in equal abundance: tetrahedrally coordinated OAl_4 sites, and hydroxyl sites, with oxygen coordinated to two aluminum ions and one hydrogen (designated Al_2OH).[22] The hydroxyl oxygens are actually coordinated to two hydrogens, the second inolved in a

(15) Walter, T. H.; Turner, G. L.; Oldfield, E. *J. Magn. Reson.* **1988**, *76*, 106.
(16) Samoson, A. *Chem. Phys. Lett.* **1985**, *119*, 29.
(17) Fukushima, E.; Roeder, S. B. W. *Experimental Pulse NMR*; Addison-Wesley: Reading, MA; 1981, pp 174–176.
(18) Avogadro, A.; Rigamonti, A. In *Magnetic Resonance and Related Phenomena*; Hovi, V., Ed.; North Holland: Amsterdam, 1973; p 255.
(19) Abragam, A. *The Principles of Nuclear Magnetism*; Oxford University: Oxford, U.K., 1961; pp 97–132.
(20) Samoson, A.; Kundla, E.; Lippmaa, E. *J. Magn. Reson.* **1982**, *49*, 350.
(21) Brun, E.; Derighetti, B.; Hundt, E. E.; Niebuhr, H. H. *Phys. Lett.* **1970**, *31A*, 416.
(22) Christoph, G. G.; Corbato, C. E., Hofmann, D. A.; Tettenhorst, R. T. *Clays Clay Mineral* **1979**, *27*, 81.

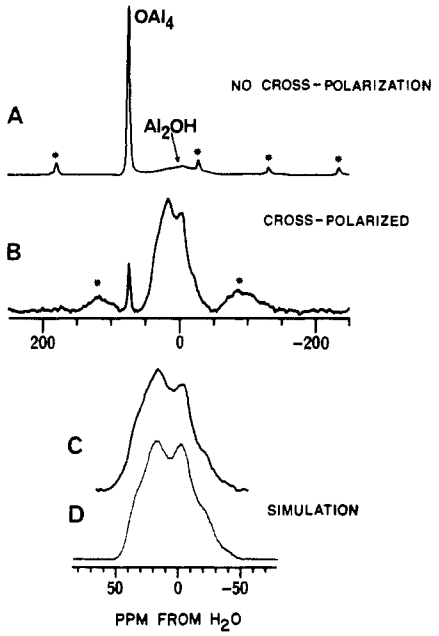

Figure 2. Oxygen-17 NMR spectra of crystalline boehmite (AlO(OH)) obtained at 68 MHz. (A) MAS spectrum with proton decoupling; 7.0 kHz spinning speed, 100 acquisitions with a 10-s recycle time (* indicates spinning sidebands). (B) CPMAS spectrum; 0.1 ms contact time, 100 acquisitions with a 2-s recycle time. (C) Expanded view of hydroxyl oxygen resonance from B. (D) Simulated spectrum using C_Q = 5.0 MHz, η = 0.5, δ_i = 40 ppm, 300 Hz line broadening.

hydrogen bond to an adjacent hydroxyl site. As shown in Figure 2A for an ^{17}O-enriched sample of crystalline boehmite, resonances from these two sites are readily resolved by using magic angle spinning, in conjunction with high-power decoupling to remove ^1H-^{17}O dipolar coupling. We have shown previously for gelatinous boehmite that the narrow resonance at 68 ppm can be assigned to the OAl_4 site, while the broader resonance at 0 ppm can be assigned to the Al_2OH site.[15] It is possible to selectively enhance the relatively weak resonance from the Al_2OH site through the use of ^{17}O–^1H cross polarization. The result of a cross-polarization experiment on crystalline boehmite is shown in Figure 2B. In contrast to the cross-polarization spectrum previously reported for gelatinous boehmite,[15] for crystalline boehmite we observe a well-defined quadrupolar line shape from the Al_2OH site, which can be closely simulated using C_Q = 5.0 MHz, η = 0.5, and an isotropic chemical shift (δ_i) of 40 ppm (see Figure 2, C and D).

In contrast to the Al_2OH resonance, the OAl_4 resonance of crystalline boehmite exhibits no quadrupolar structure, so that the quadrupole coupling parameters cannot be obtained by direct simulation. An alternative method for estimating C_Q, but not η, exploits the fact that the resonances of quadrupolar nuclei are shifted from their true chemical shift values, δ_i, as a result of the quadrupolar interaction.[16] For ^{17}O, the difference between the observed chemical shift of the main (1/2, −1/2) resonance, $\delta_{obs}(1/2)$, and δ_i is given by

$$\delta_{obs}(1/2) - \delta_i = -6000(C_Q/\nu_L)^2(1 + \eta^2/3)$$

where ν_L is the Larmor frequency. Similarly, the difference between the observed chemical shifts of the (±3/2, ±1/2) transitions, $\delta_{obs}(3/2)$, and δ_i, is given by

$$\delta_{obs}(3/2) - \delta_i = 750(C_Q/\nu_L)^2(1 + \eta^2/3)$$

The difference between $\delta_{obs}(1/2)$ and $\delta_{obs}(3/2)$, the latter being measured by taking the average over the positions of the high order (>1) spinning sidebands, is thus given by

$$\delta_{obs}(3/2) - \delta_{obs}(1/2) = 6750(C_Q/\nu_L)^2(1 + \eta^2/3)$$

Assuming η = 0, which causes at most a 15% error, this method yields C_Q = 1.2 MHz and δ_i = 70 ppm for the OAl_4 site of crystalline boehmite.

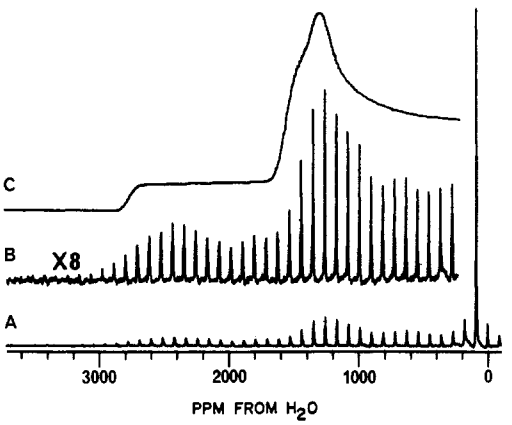

Figure 3. Oxygen-17 NMR spectrum of crystalline boehmite showing spinning sidebands from satellite transitions. (A) MAS spectrum at 68 MHz; 6.0 kHz spinning speed, 600 acquisitions with a 2.5-s recycle time. (B) Vertical expansion of A showing spinning sidebands. (C) Simulated spectrum showing powder line shape for (3/2, 1/2) and (−1/2, −3/2) transitions, using C_Q = 1.2 MHz, η = 0.10, 3500 Hz line broadening.

Another way of obtaining quadrupole coupling parameters for this site is to examine the spinning sideband intensities over a wide spectral width.[23] As shown in Figure 3, spinning sidebands can be detected over a range of 3000 ppm (ca. 200 kHz) on both sides of the centerband resonance. Only half the pattern is shown, the full spectrum being symmetric about the centerband. These spinning sidebands arise from the (3/2, 1/2) and (−1/2, −3/2) transitions, which are not normally observed for ^{17}O, or other noninteger spin quadrupolar nuclei, because they extend over a much wider region than the (1/2, −1/2) transition. We observe no spinning sidebands from the (5/2, 3/2) and (−3/2, −5/2) transitions, which would be shifted by 6.6 ppm from the (±3/2, ±1/2) transition sidebands, apparently due to their much weaker intensity and 6-fold greater line width.[20] As shown in Figure 3B, the intensity envelope of the spinning sidebands can be fit to a (±3/2, ±1/2) first-order quadrupolar line shape having C_Q = 1.20 MHz and η = 0.1. Thus we can obtain not only a more accurate determination of the quadrupole coupling constant for this site, but also an estimate of the asymmetry parameter. Although this method is useful for this particular case, it is not as generally applicable as the quadrupole shift method since it requires precise setting of the magic angle (to avoid broadening of the spinning sidebands), very stable spinning frequencies (to within ca. 5 Hz), and high signal-to-noise ratios (since the sidebands are an order of magnitude less intense than the centerband resonance).

Al(OH)$_3$. Aluminum hydroxide occurs in three forms: gibbsite, bayerite, and norstrandite. All three forms are built up from sheets of edge-sharing $Al(OH)_6$ octahedra and differ mainly in the stacking of these sheets.[24] In all forms there is only a single type of oxygen environment, an Al_2OH site with C_s symmetry. However, it is known that several crystallographically inequivalent oxygen sites are present in each form, with bayerite having three distinct sites.[25] We show in Figure 4A the MAS ^{17}O NMR spectrum of ^{17}O-enriched bayerite obtained with high-power proton decoupling. The narrow resonance at 68 ppm arises from a small amount of gelatinous boehmite in the sample, while the broader resonance arises from the bayerite. The latter resonance exhibits a second-order quadrupolar line shape that can be simulated moderately well by using a single powder pattern with C_Q = 6.0 MHz, η = 0.5, and δ_i = 40 ppm (see Figure 4, B and C). We note, however, that the unusual broadness of this resonance appears to indicate that the three crystallographically inequivalent oxygen sites may have slightly different quadrupole coupling parameters, in which case the observed line shape could consist of three overlapping powder patterns. There is clearly not enough structure

(23) Clayden, N. J. *Chem. Scri.* **1987**, *28*, 211.
(24) Schoen, R.; Roberson, C. E. *Am. Mineral.* **1970**, *55*, 43.
(25) Rothbauer, V. R.; Zigan, F.; O'Daniel, H. *Z. Kristallogr.* **1967**, *125*, 317.

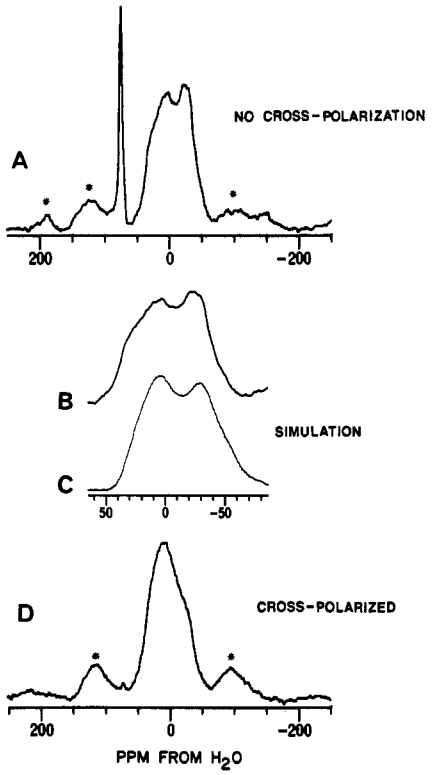

Figure 4. Oxygen-17 NMR spectra of bayerite ($Al(OH)_3$) obtained at 68 MHz. (A) MAS spectrum with proton decoupling; 7.6 kHz spinning speed, 180 acquisitions with a 10-s recycle time (* indicates spinning sidebands). (B) Expanded view of A. (C) Simulated spectrum using C_Q = 6.0 MHz, η = 0.3, δ_i = 40 ppm, 500 Hz line broadening. (D) CPMAS spectrum; 6.5 kHz spinning speed, 1 ms contact time, 640 acquisitions with a 5-s recycle time.

in the spectrum of Figure 4B to afford a unique three-component simulation. As shown in Figure 4D, under cross-polarization conditions the quadrupolar line shape appears somewhat distorted, with the low-field singularity being enhanced relative to the high-field singularity. This is apparently due to the anisotropic cross-relaxation effect noted previously for $Mg(OH)_2$ and $Ca(OH)_2$.[15] Although this distortion becomes less prominent at longer contact times, the short (ca. 1.5 ms) $T_{1\rho}$ of this site impedes the use of the long contact times required to obtain an undistorted spectrum.

γ-Al_2O_3. While the structures of the transitional aluminas are not as well-defined as those of their aluminum hydroxide precursors or α-Al_2O_3, X-ray powder diffraction indicates that the γ- and η-Al_2O_3 lattices are closely related to that of spinel ($MgAl_2O_4$).[1] The unit cell of spinel is built up from a cubic close-packed array of 32 oxide ions, with 16 Al^{3+} ions in octahedral holes and 8 Mg^{2+} ions in tetrahedral holes.[26] In the transitional aluminas, electroneutrality requires that only $21\frac{1}{3}$ Al^{3+} ions be distributed over these 24 cation positions, leaving $2\frac{2}{3}$ holes vacant per unit cell. The differences between the various transitional aluminas are primarily due to differences in the locations and ordering of these vacancies in the lattice. The spinel structure contains a single oxygen site, with oxygen coordinated to three aluminum atoms and one magnesium atom.[26] The corresponding oxygen site in the transitional aluminas is an OAl_4 site, where three of the neighboring aluminum atoms are octahedrally coordinated and the remaining one is tetrahedrally coordinated. The effect on the local oxygen environment produced by cation vacancies will be that some trigonally coordinated (OAl_3) oxygen sites must also exist.

We show in Figure 5A the ^{17}O MAS NMR spectrum of a high surface area (180 m^2/g) γ-Al_2O_3 sample prepared by dehydrating ^{17}O-enriched gelatinous boehmite at 500 °C. The spectrum shows

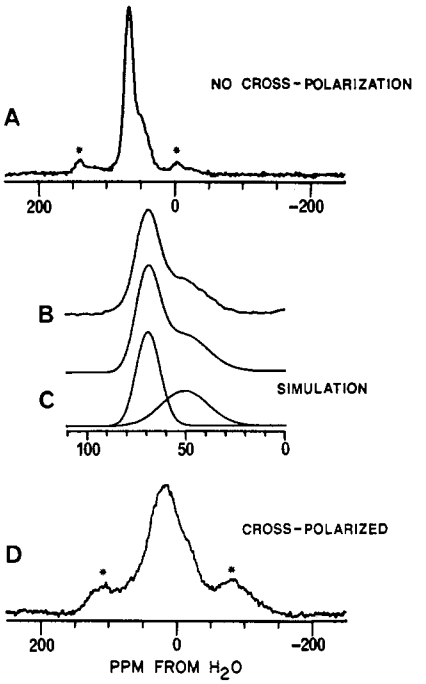

Figure 5. Oxygen-17 NMR spectra of γ-Al_2O_3 made from gelatinous boehmite, obtained at 68 MHz. (A) MAS spectrum with proton decoupling; 5.0 kHz spinning speed, 5500 acquisitions with a 1-s recycle time (* indicates spinning sidebands). (B) Expanded view of A. (C) Simulated spectrum using two Gaussian line shapes in a 1:1 ratio, with line widths of 950 and 1830 Hz. (D) CPMAS spectrum with proton decoupling; 6.7 kHz spinning speed, 0.1 ms contact time, 10 000 acquisitions with a 2 sec recycle time.

two overlapping resonances near 70 ppm, with line widths of ca. 900 and 1800 Hz. Simulation of this spectrum as the sum of two Gaussian resonances, as illustrated in Figure 5B,C, indicates that the ratio of the integrated intensities of the two resonances is approximately 1:1. We assign the narrower resonance to the OAl_4 sites and the broader peak to the trigonal OAl_3 sites. The greater breadth of this latter resonance is attributed to a larger quadrupole coupling constant for these trigonal sites, although we cannot discern any second-order quadrupolar splitting in the line shape. This is apparently due to the disordered nature of the γ-Al_2O_3 structure, producing a distribution of bond angles and distances, and hence quadrupole coupling parameters, for each type of oxygen environment. While the relatively narrow OAl_4 resonance also shows no sign of quadrupolar splitting, we can use the quadrupole shift method described above to determine that this site has a quadrupole coupling constant of ca. 1.8 MHz, assuming η = 0. The spinning sideband pattern observed for this site is consistent with this estimate of the quadrupole coupling constant, although it does not appear to trace out a well-defined powder line shape, again indicating a disordered structure.

Surface Hydroxyls. The spectrum of Figure 5A shows no features attributable to the ca. 13% of the oxygens present as hydroxyls groups, based on the measured BET surface area of 180 m^2/g and an area of 8 $Å^2$ per hydroxyl group.[27] However, these hydroxyl sites can be observed by using ^{17}O–^1H cross polarization, as shown in Figure 5D. Despite the signal-to-noise enhancement provided by cross polarization, the relative scarcity of these hydroxyl groups necessitates extensive signal averaging to achieve a moderate signal-to-noise ratio. Estimating a cross polarization enhancement factor of 3, a typical value for the hydroxyl sites of bayerite and boehmite, we find that the hydroxyl oxygen resonance is only ca. 10% as intense as the non-hydroxyl oxygen resonances, so that the hydroxyls represent 9% of the total intensity. Although this value can only be considered an estimate, owing to uncertainty in the cross polarization enhancement factor, it is in reasonable agreement with the 13% value calculated for

(26) Hill, R. J.; Craig, J. R.; Gibbs, G. V. *Phys. Chem. Minerals* **1979**, *4*, 317.

(27) Peri, J. B. *J. Phys. Chem.* **1965**, *69*, 220.

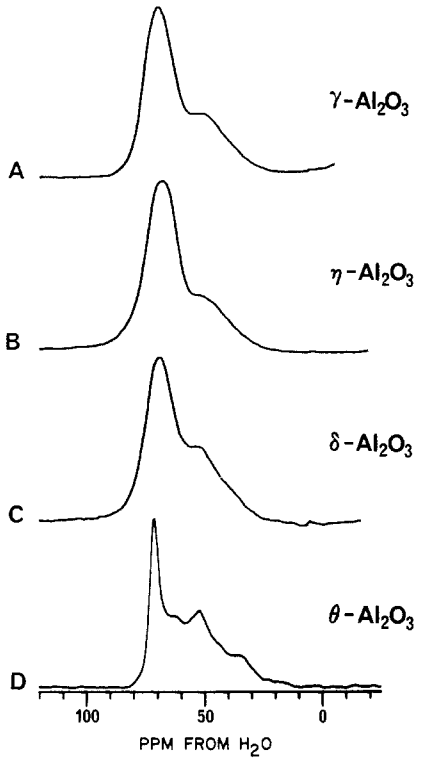

Figure 6. Oxygen-17 NMR spectra of several transitional aluminas obtained at 68 MHz. (A) γ-Al_2O_3 prepared by dehydrating crystalline boehmite at 500 °C for 5 h; 100 acquisitions with a 5-s recycle time: (B) η-Al_2O_3 prepared by dehydrating bayerite at 400 °C for 11 h; 100 acquisitions with a 5-s recycle time. (C) δ-Al_2O_3 prepared by dehydrating crystalline boehmite at 850 °C for $2^1/_2$ h; 500 acquisitions with a 30 sec recycle time. (D) θ-Al_2O_3 prepared by dehydrating bayerite at 950 °C for $3^1/_2$ h; 500 acquisitions with a 30-s recycle time.

a fully hydroxylated surface. The actual hydroxyl concentration should be less than 13%, as we observe, since some dehydroxylation occurs as the γ-Al_2O_3 is formed at 500 °C.

Although the resonance of Figure 5D shows little evidence of quadrupolar fine structure, it closely resembles the hydroxyl oxygen resonance observed for bayerite under cross-polarization conditions (see Figure 4D). It is known that different types of hydroxyl sites are present on the surfaces of transitional aluminas.[6] Based on the assumption that undistorted low-index crystal faces are exposed, Knozinger and Ratnasamy have identified five possible types of hydroxyl groups on γ- and η-Al_2O_3:[6]

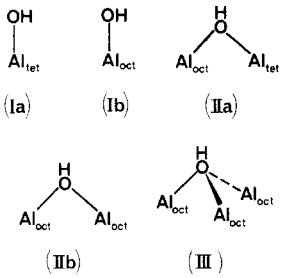

Site IIb, in which the hydroxyl oxygen is coordinated to two octahedral aluminum cations, is similar to the hydroxyl sites of bayerite and boehmite. In the crystalline aluminum hydroxides, however, a second proton is coordinated to the hydroxyl oxygen in a hydrogen bond to an adjacent hydroxyl site. The similarity of the surface hydroxyl resonance of γ-Al_2O_3 and the resonance from the Al_2OH site of bayerite suggests that site IIb could be the dominant type of hydroxyl group in this γ-Al_2O_3 sample. This would be in agreement with the observation that sites IIa and IIb should dominate, based on the preferential exposure of the (111)-plane in γ-Al_2O_3.[6] Hydroxyl types Ia and Ib are expected to have relatively large ^{17}O quadrupole coupling constants, based on a point charge model for calculating electric field gradients

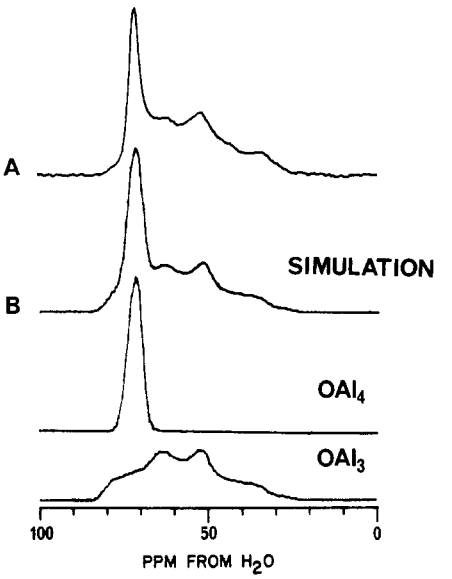

Figure 7. Oxygen-17 NMR spectra of θ-Al_2O_3 obtained at 68 MHz. (A) Expanded view of Figure 6D. (B) Simulated spectrum using two components in a 1:2 ratio: (i) C_Q = 1.2 MHz, η = 0.0, δ_i = 72 ppm, 125 Hz line broadening. (ii) C_Q = 4.0 MHz, η = 0.6, δ_i = 79 ppm, 125 Hz line broadening.

(vide infra). However, a similar calculation for hydroxyl type III indicates that this site should also have an ^{17}O quadrupole coupling constant comparable to that of the type II sites. Thus it is possible that type III sites may contribute to the resonance of Figure 5D, in addition to type II sites.

Comparison between Transitional Aluminas. We show in Figure 6 a comparison of the ^{17}O MAS NMR line shapes of γ-, η-, δ-, and θ-Al_2O_3. As described above, all of the transitional aluminas are believed to have similar structures, differing mainly in the ordering of the aluminum vacancies.[1] It can be seen from Figure 6 that, with the exception of θ-Al_2O_3, this cation ordering produces relatively subtle differences in the ^{17}O NMR spectra. The spectra of η- and δ-Al_2O_3 are very similar to that of γ-Al_2O_3, showing two overlapping resonances with line widths of ca. 900 and 1800 Hz, attributed to OAl_4 and OAl_3 sites, respectively. Using the quadrupole shift method, we calculate quadrupole coupling constants of 1.6 MHz for the OAl_4 sites of both η- and δ-Al_2O_3, and isotropic chemical shifts of 73 and 72 ppm, respectively. For the OAl_4 site of θ-Al_2O_3, we obtain C_Q = 1.2 MHz and δ_i = 72 ppm. Because of their greater line width, we are unable to obtain quadrupole coupling constants for the OAl_3 sites using this method. However, it can be seen in Figure 6 that while the OAl_3 resonances of the two low-temperature aluminas (γ and η) have nearly Gaussian line shapes, presumably due to a broad distribution of quadrupole coupling parameters, the OAl_3 resonances of the high-temperature aluminas (δ and θ) are distinctly non-Gaussian, showing some indications of quadrupolar structure. This is consistent with the more ordered structures of the high-temperature forms, as evidenced by the sharpness of their powder X-ray diffraction spectra.[1] While the OAl_3 resonance of δ-Al_2O_3 is too ill-defined to simulate, that of θ-Al_2O_3 exhibits a well-defined quadrupolar line shape. θ-Al_2O_3 is known to be highly ordered, with a structure isomorphous with that of β-Ga_2O_3.[28] The β-Ga_2O_3 structure has three oxygen sites, including one tetrahedral site, and two distinct trigonal sites. These sites may be designated as $OGa^o_3Ga^t$, $OGa^o_2Ga^t$, and $OGa^oGa^t_2$, where Ga^o and Ga^t represent gallium in octahedral and tetrahedral coordination, respectively.[29] As illustrated in Figure 7, the spectrum of θ-Al_2O_3 can be closely simulated by using only two second-order quadrupolar line shapes, the two trigonal oxygen sites being indistinguishable. The resonance from the OAl_3 oxygen sites, which has approximately twice the integrated intensity of the OAl_4 resonance,

(28) Saalfeld, H. *Neues Jahrb. Mineral., Abh.* **1960**, *95*, 1.
(29) Geller, S. *J. Chem. Phys.* **1960**, *33*, 676.

can be fit by using C_Q = 4.0 MHz, η = 0.6, and δ_i = 79 ppm.

Calculation of Quadrupole Coupling Parameters. It has previously been shown that ^{17}O quadrupole coupling constants are strongly correlated with the relative ionic character of the bonds to oxygen, with predominantly ionic bonding being associated with small coupling constants.[9] This correlation arises because covalent bonding disrupts the spherical symmetry of the O^{2-} ion, producing large electric field gradients at the oxygen nucleus. Using Pauling's electronegativities to estimate the relative ionic character of Al–O and O–H bonds, the Schramm and Oldfield correlation[9] predicts quadrupole coupling constants of 2.0 and 4.8 MHz for Al–O–Al and Al–O–H fragments, respectively. While these predictions are in agreement with our observation of larger coupling constants for Al_2OH sites relative to OAl_4 sites, they give no indication of the factors that are responsible for differences in the quadrupole coupling parameters of similar sites in different compounds. To gain some insight into the relationship between structure and quadrupole coupling parameters, we have used the point monopole model to estimate the electric field gradients (V_{ij}; $i,j = x, y, z$) at the oxygen sites produced by the ionic lattice. The elements of the electric field gradient (efg) tensor produced at an oxygen site by an ion of charge ζe are given by

$$V_{ij} = -(1/4\pi\epsilon_0)\zeta e|\mathbf{r}|^{-5}(3r_ir_j - |\mathbf{r}|^2\delta_{ij}) \quad (1)$$

where $\mathbf{r}$ is the radius vector from the oxygen nucleus to the ion and δ_{ij} is the Kronecker delta.[30] This calculation completely neglects covalency, and is thus useful for predominantly ionic solids, such as Al_2O_3. For more covalent cases, the Townes-Dailey formalism has been shown to be appropriate.[10,13] In calculating the electric field gradient tensor at an oxygen site in a crystal lattice, the contributions from each ion in the lattice must be summed. In practice, we find that the tensor elements can be estimated to within better than 5% by carrying out the summation for a neutral crystal fragment extending out 50 Å from the oxygen site under consideration. As a check on the accuracy of these calculations, we note that our results for α-Al_2O_3 (V_{zz} = 1.18 × 10^{21} V/m^2) are in agreement with the more rigorous multipole lattice sum calculations of Hafner and Raymond (V_{zz} = 1.12 × 10^{21} V/m^2).[31]

In general, the efg tensor obtained by this point charge calculation must be diagonalized to obtain the principal components V_{xx}, V_{yy}, and V_{zz}. By convention, $|V_{zz}| > |V_{yy}| > |V_{xx}|$. The observables, C_Q and η, are related to these by

$$C_Q = (1 - \gamma_\infty)eQV_{zz}/h$$

$$\eta = (V_{xx} - V_{yy})/V_{zz}$$

where Q is the nuclear quadrupole moment (−0.0265 × 10^{-24} cm^2 for ^{17}O) and γ_∞ is the Sternheimer antishielding factor. Although η can be calculated directly from the efg tensor, calculation of the quadrupole coupling constant requires an estimate of γ_∞, which accounts for distortions induced in the core electrons by the external field gradients.[32] Unfortunately, there is little agreement among the γ_∞ values calculated for oxide ions in crystal lattices, with theoretical values ranging from −28.2[33] to −13.785.[34] The inadequacy of these calculated values is indicated by the fact that they lead to quadrupole coupling constants that are an order of magnitude larger than the experimental values. For example, using γ_∞ = −25.4, Hafner and Raymond calculated C_Q = 18.9 MHz for the oxygen site of α-Al_2O_3,[31] while the experimental value is only 2.17 MHz. We can obtain an estimate of γ_∞ for oxygen in aluminum oxides and hydroxides by plotting the observed quadrupole coupling constants vs the calculated V_{zz} values. As shown in Figure 8, such a plot for the oxygen sites in α-Al_2O_3, bayerite, and crystalline boehmite is indeed linear. Omitting the OAl_4 site of boehmite, the remaining three points yield a correlation coefficient of 0.9996, with a slope of 2.05 × 10^{-15} m^2/(V s), giving γ_∞ = −2.20. The C_Q values calculated by using this value for the antishielding factor are given in Table II, along with the calculated asymmetry parameters.

TABLE II: Calculated Oxygen-17 Nuclear Quadrupole Coupling Constants and Electric Field Gradient Asymmetry Parameters for Aluminum Oxides and Hydroxides

system	struct ref	site	C_Q, MHz	η
α-Al_2O_3	5	OAl_4	2.41	0.62
AlO(OH) (boehmite)	22	OAl_4	1.83	0.27
		Al_2OH	5.17	0.25
$Al(OH)_3$ (bayerite)	25	Al_2OH	6.27	0.26
β-Ga_2O_3	29	$OGa^o_3Ga^t$ [a]	1.73	0.18
		$OGa^oGa^t_2$	3.52	0.02
		$OGa^o_2Ga^t$	2.51	0.94

[a] Ga^o represents Ga in octahedral coordination, Ga^t in tetrahedral coordination.

It can be seen by comparing the values in Tables I and II that the point charge calculation provides a satisfactory account of the asymmetry parameters and relative quadrupole coupling constants for the OAl_4 site in α-Al_2O_3 and the Al_2OH sites in boehmite and bayerite. While the agreement is not as satisfactory for the OAl_4 site of boehmite, the point charge model does correctly indicate both the smaller C_Q and η values of this site relative to the OAl_4 site of α-Al_2O_3. The smaller quadrupole coupling constant and asymmetry parameter of the OAl_4 site in boehmite are not due to a more nearly tetrahedral arrangement around the oxygen atom, as might be expected based on previous correlations between C_Q and polyhedral distortion.[35,36] In fact, the bond angle variance, σ_θ^2, a measure of the deviations of the AlOAl bond angles (θ) from the ideal tetrahedral value of 109.47°:[37]

$$\sigma_\theta^2(\text{tet}) = \sum_{i=1}^{6}(\theta_i - 109.47°)^2/5$$

is larger for the OAl_4 site of boehmite (σ_θ^2 = 589.5) than for α-Al_2O_3 (σ_θ^2 = 454.0). Thus the smaller quadrupole coupling constant and asymmetry parameter of the OAl_4 site of boehmite relative to that of α-Al_2O_3 cannot be accounted for simply, being due to relatively subtle differences between the two structures.

In addition to quadrupole coupling constants and asymmetry parameters, the point monopole calculations also yield the orientation of the efg tensors relative to the crystal lattice, and hence to the molecular coordinate system. The orientation of the principal axis system of the calculated efg tensor for the OAl_4 site of α-Al_2O_3 is shown in Figure 9A. The Z axis is perpendicular to the bisector of the largest Al–O–Al angle, while the X axis coincides with the C_2 axis. With this orientation, the Z axis forms a 44° angle with respect to the crystal c axis, in agreement with the value of 45.85° determined by Brun et al. for a single crystal of ruby (Al_2O_3:Cr^{3+}).[21] The calculated efg tensor principal axis system for the OAl_4 site of boehmite has a similar orientation. Again, the x axis coincides with the C_2 symmetry axis, while the Z axis is perpendicular to the bisector of the largest Al–O–Al angle, this time lying in the Al–O–Al plane, as required by the C_{2v} site symmetry.

As evident from Figure 8, the point charge model correctly yields larger quadrupole coupling constants for the Al_2OH sites relative to the OAl_4 sites. In the point charge efg formalism, the large electric field gradients at the hydroxyl oxygens are primarily due to the short (ca. 1 Å) O–H bonds. In both boehmite and

(30) Cohen, M. H.; Reif, F. In *Solid State Physics, Advances in Research and Applications*; Seitz, F., Turnbull, D., Eds; Academic: New York, 1957; p 321.
(31) Hafner, S.; Raymond, M. *J. Chem. Phys.* **1968**, *49*, 3570.
(32) Lucken, E. A. C. *Nuclear Quadrupole Coupling Constants*; Academic: London, 1969; p 79.
(33) Burns, G. Wikner, E. G. *Phys. Rev.* **1961**, *121*, 155.
(34) Schmidt, P. C.; Sen, K. D.; Das, T. P.; Weiss, A. *Phys. Rev. B* **1980**, *22*, 4167.
(35) Ghose, S.; Tsang, T. *Am. Mineral.* **1973**, *58*, 748.
(36) Turner, G. L.; Chung, S. E.; Oldfield, E. *J. Magn. Reson.* **1985**, *64*, 316.
(37) Robinson, K.; Gibbs, G. V.; Ribbe, P. H. *Science* **1971**, *172*, 567.

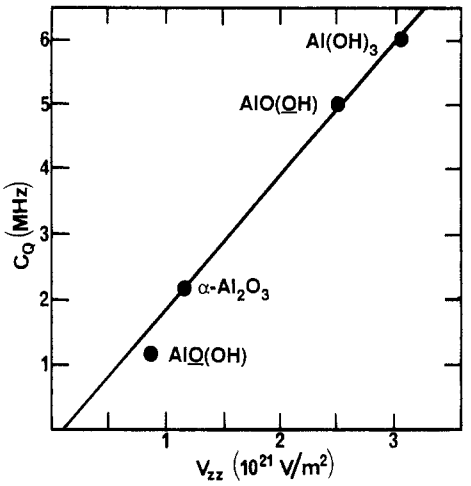

Figure 8. Plot of experimental ^{17}O quadrupole coupling constants vs calculated electric field gradient (V_{zz}). The solid line shows the least-squares fit, omitting the point representing the OAl_4 site of boehmite.

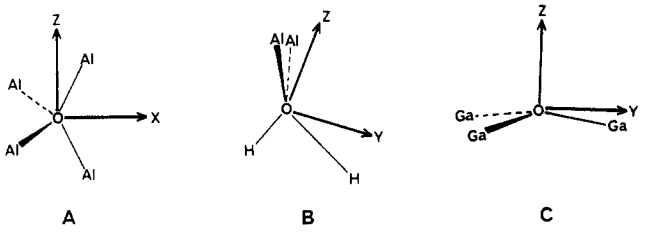

Figure 9. Principal axis systems of the calculated ^{17}O electric field gradient tensors of representative oxygen sites. (A) OAl_4 site in α-Al_2O_3. (B) Al_2OH site in boehmite. (C) $OGa^oGa^t_2$ site in β-Ga_2O_3.

bayerite, the hydroxyl oxygen sites actually have two proton nearest neighbors, due to the hydrogen bonding between adjacent sites. Unfortunately, the hydrogen positions in boehmite are not accurately known, so we have estimated them using the asymmetric hydrogen bond model proposed to account for the results of ^1H NMR second-moment measurements.[38] These positions are similar to those determined for the isomorphous FeO(OH) polymorph, lepidocrocite.[39] Using the asymmetric hydrogen bond structure, we calculate $C_Q = 5.17$ MHz, $\eta = 0.25$ for the hydroxyl oxygen site of boehmite, in good agreement with the experimental values of 5.0 MHz and 0.5, respectively. Calculations based on the alternative symmetric hydrogen bond model yield a significantly larger quadrupole coupling constant (6.59 MHz) and a smaller asymmetry parameter (0.08). The agreement between the experimental quadrupole coupling parameters and the values calculated based on the asymmetric hydrogen bonding model thus provides further support for asymmetric hydrogen bonds in boehmite. The orientation of the calculated efg tensor principal axis system for this site is shown in Figure 9B. The X axis is perpendicular to the mirror plane, while the Z axis is in the H–O–H plane, tilted by 9° from the short O–H bond direction. The calculated efg principal axes are similarly oriented for the Al_2OH site of bayerite, although this site lacks the symmetry plane of the hydroxyl oxygen site in boehmite. Again, the Z direction nearly coincides with the direction of the short O–H bond, deviating by 12° in this case. The point charge calculation correctly yields the larger quadrupole coupling constant of this site relative to the hydroxyl site of boehmite, this difference being primarily due to the slightly shorter O–H bond length in bayerite (0.95 Å, vs 0.98 Å in boehmite). The values for bayerite were calculated for only the 0,2 site in the powder diffraction refinement of Rothbauer et al.[25] For the other two oxygen sites in this refinement, the O–H bond lengths appear to be unreasonably short[40] (0.82 and 0.77 Å) and consequently give rise to large quadrupole coupling constants (11.5 and 12.6 MHz).

Although it has not been possible to obtain an accurate structure determination for any of the transitional aluminas, the structure of β-Ga_2O_3, which is believed to be isomorphous with θ-Al_2O_3, is known.[29] The calculated quadrupole coupling parameters for the three oxygen sites of β-Ga_2O_3 are given in Table II. Because the Ga–O bonds in β-Ga_2O_3 are ca. 4% longer than the Al–O bonds in θ-Al_2O_3,[28] the coupling constants for θ-Al_2O_3 should be larger than those of β-Ga_2O_3 by ca. 12%, owing to the r^{-3} dependence of the electric field gradients. The calculations for β-Ga_2O_3 thus indicate a quadrupole coupling constant of 1.9 MHz for the OAl_4 site of θ-Al_2O_3, somewhat larger than the experimental value of 1.2 MHz. For the trigonal oxygen sites of θ-Al_2O_3, the β-Ga_2O_3 calculations indicate quadrupole coupling constants of 3.9 and 2.8 MHz, with asymmetry parameters of 0.02 and 0.94, respectively. The orientation of the principal axes of the calculated efg tensor for one of the trigonal oxygen sites (the $OGa^oGa^t_2$ site) in β-Ga_2O_3 is shown in Figure 9C. The Z axis is perpendicular to the plane containing the three gallium atoms, while the Y axis is parallel to that plane, bisecting one of the Ga–O–Ga bonds. The asymmetry parameter for this site is very small, as a result of its nearly 3-fold symmetry. The orientation of the principal axis system for the second trigonal oxygen site (the $OGa^o_2Ga^t$ site) is similar, although the greater deviation from 3-fold symmetry produces a much larger asymmetry parameter. The observation that the ^{17}O NMR spectrum of θ-Al_2O_3 is well fit using only one trigonal oxygen line shape suggests that its structure is significantly different from that of β-Ga_2O_3. Nevertheless, the observed quadrupole coupling constant of 4.0 MHz for the trigonal oxygens of θ-Al_2O_3 is similar to the values calculated for a structure isomorphous with β-Ga_2O_3. The experimental asymmetry parameter of 0.6 indicates that the OAl_3 sites of θ-Al_2O_3 deviate to a large extent from 3-fold symmetry.

Conclusions

The results described above show that ^{17}O NMR can provide new information on the structures of aluminum oxides and hydroxides. It is interesting to compare the information provided by ^{17}O NMR with that provided by ^{27}Al NMR of the same materials. All of the aluminum hydroxides and oxide hydroxides, as well as α-Al_2O_3, contain aluminum in octahedral coordination. Consequently, all of these phases yield a single featureless ^{27}Al resonance near 0 ppm.[41] In contrast, the ^{17}O NMR spectra of the well-defined aluminum oxides and hydroxides are quite distinct. For example, ^{17}O NMR clearly reveals the presence of both oxide and hydroxide sites in boehmite. Furthermore, the ^{17}O quadrupole coupling parameters are different for each site, providing a sensitive probe of the local structure.

In contrast to the generally uninformative spectra of the well-defined phases, ^{27}Al NMR spectra of transitional aluminas show the presence of aluminum in both tetrahedral and octahedral coordination.[7,8] However, ^{27}Al NMR reveals few differences among the transitional aluminas. Oxygen-17 NMR, however, clearly indicates the greater order of the high-temperature transitional aluminas relative to the low-temperature forms, with the spectrum of θ-Al_2O_3 exhibiting well-defined line shapes from both the OAl_4 and OAl_3 oxygen sites. We have also shown that ^{17}O cross-polarization NMR allows the direct observation of hydroxyl groups on the surfaces of transitional aluminas. Analysis of the line shape for the hydroxyl resonance of γ-Al_2O_3 suggests that the predominant type of hydroxyl is a type IIb Al_2OH site, similar to the hydroxyl sites in bayerite. Using ^{17}O NMR, it may be possible to examine how the surface structure of alumina is affected by the attachment of metal complexes or crystallites,

(38) Holm, C. H.; Adams, C. R.; Ibers, J. A. *J. Phys. Chem.* **1958**, *62*, 992.

(39) Christensen, H.; Christensen, A. N. *Acta Chem. Scand. A* **1978**, *32*, 87.

(40) For a collection of O–H bond distances, see: Hamilton, W. C.; Ibers, J. A. *Hydrogen Bonding in Solids*; W. A. Benjamin: New York, 1968; pp 259–265.

(41) Kinsey, R. A. Ph.D. Thesis, University of Illinois at Urbana-Champaign, 1985.

perhaps providing some insight into the nature of metal–support interactions.

Acknowledgment. This work was supported in part by the U.S. National Science Foundation Solid State Chemistry Program (grant DMR 86-15206). We thank B. Phillips for the use of his electric field gradient calculation program and for obtaining powder X-ray diffraction spectra, C. Weiss for assistance with the synthesis of crystalline boehmite, Dr. A. Irwin for the surface area measurement, and Dr. A. Thompson and Dr. G. Turner for helpful discussions.

Registry No. Al_2O_3, 1344-28-1; AlO(OH), 24623-77-6; $Al(OH)_3$, 21645-51-2; ^{17}O, 13968-48-4; boehmite, 1318-23-6; bayerite, 20257-20-9.

Orientation of Caroviologens in Model Membranes

L. B.-Å. Johansson,*,† M. Blanchard-Desce,‡ M. Almgren,§ and J.-M. Lehn‡

Department of Physical Chemistry, University of Umeå, S-901 87 Umeå, Sweden, Chimie des Interactions Moléculaires, Collège de France, 11 Place Marcelin Berthelot, 75005 Paris, France, and The Institute of Physical Chemistry, University of Uppsala, P.O. Box 532, S-751 21 Uppsala, Sweden
(Received: December 15, 1988)

The bis(4-pyridinium) polyenes, called caroviologens, are of potential interest as devices for electron transfer by a molecular wire-type process. The orientation of three caroviologens (denoted by 1^{2+}, 2^{2+}, and 3^{2+}) solubilized in five different lipid model membranes was studied by means of polarized electronic absorption spectroscopy. The model membranes were macroscopically aligned, and the dichroic ratio of the electronic spectrum was determined in the wavelength region 350–700 nm. It is found that the orientation of the caroviologens depends on the length of the polyene chain as well as the thickness of the lipid bilayer. If the long axis of the caroviologen exceeds or matches the thickness of a lipid bilayer, the long axis of the molecule is oriented preferentially perpendicular to the membrane.

Introduction

Molecular wires that would allow an electron flow between different molecules are of great interest in the design of molecular devices.[1-3] The caroviologens, which are potential candidates for such molecular wires, combine the properties of the carotenoids and of the viologens: The pyridinium group of the viologens is water soluble and electroactive for electron exchange, while the nonpolar conjugated polyene chain conducts electrons efficiently. The solubility properties are typical of amphiphile molecules, and the caroviologens should dissolve in lipid bilayers. Depending on the orientation of the caroviologen in a membrane it may more or less efficiently serve as a conductor of electrons across or along the bilayer.

This work aims at investigating the orientational dependence of the caroviologens on their length and on the thickness of the bilayer. Three caroviologens denoted by 1^{2+}, 2^{2+}, and 3^{2+} (see Figure 1) were studied. The thickness of the lipid model membranes was varied from about 20 to 40 Å.

Materials and Methods

The bis(4-pyridinium) polyenes 1^{2+}, 2^{2+}, and 3^{2+} (see Figure 1) were synthesized as described in ref 1. The lipids 1-oleoyl monoglyceride and 1,2-dioleoyl-*sn*-glycero(3)phosphocholine (DOPC) were purchased from Aktieselskabet Grindstedvaerket, Grindstedt, Denmark, and Avanti Polar Lipids, Inc., respectively. 1-Octyl monoglyceride was synthesized at Syntestjänst, Chemical Centre in Lund, Sweden. Penta(ethylene glycol) mono-*n*-dodecyl ether ($C_{12}EO_5$) was obtained from Nikko Chemicals Ltd., Tokyo, Japan. Sodium octanoate from BDH was purified by filtering a solution of the amphiphile in methanol and active coal.

The lamellar liquid crystals were prepared as described in ref 4 with a molar ratio of lipid/chromophore varying between 10^3 and 10^4. At molar ratios of about 10^2, the systems contain crystals and are then most likely saturated with respect to the caroviologens. The lamellar phases were composed of sodium octanoate/1-decanol/water in the amounts 11.9/28.1/60.0 wt %, octyl monoglyceride/water in the amounts 70.0/30.0 wt %, $C_{12}EO_5$/water in the amounts 69.0/31.0 wt %, oleoyl monoglyceride/water in the amounts 90.0/10.0 wt %, and DOPC/water in the amounts 80.0/20.0 wt %. The refractive index values of the lamellar phases containing sodium octanoate, octyl monoglyceride, $C_{12}EO_5$, oleoyl monoglyceride, and DOPC are 1.40, 1.42, 1.43, 1.47, and 1.47, respectively, as obtained with an Abbe refractometer.

The macroscopical alignment of the lamellar phases was checked by observing the samples when placed between two crossed polarizers. The dichroic ratio of the electronic spectra were recorded on a Varian Cary 219 absorption spectrometer supplemented with sheet polarizers (Model HNP'B, Polarizers, Ltd.). The samples were thermostated within 293 ± 1 K.

Theoretical Prerequisites

Lamellar liquid crystals containing small amounts of chromophores can be macroscopically aligned between quartz plates.[4-6] The lamellae align with their planes parallel to the quartz plates. These systems are uniaxially anisotropic, and the optical axis and the director of the membranes coincide with the normal to the quartz plates. By shining linearly polarized light with its polarization at the angles ω and 90° ($\perp$) relative to the optical axis, the absorbances A_ω and $A_\perp$ were measured.

From the dichroic ratio $D = A_\omega/A_\perp$, information about the molecular orientation of the chromophores can be calculated from[6,7]

$$D = 1 + \frac{3S\cos^2\omega}{(1-S)n^2} \quad (1)$$

$$S = \frac{\langle 3\cos^2\beta - 1\rangle}{2} \quad (2)$$

† University of Umeå.
‡ Collège de France.
§ University of Uppsala.

(1) Arrhenius, T. S.; Blanchard-Desce, M.; Dvolaitzky, M.; Lehn, J.-M.; Malthete, J. *Proc. Natl. Acad. Sci. U.S.A.* **1986**, *83*, 5355.
(2) Lehn, J.-M. *Angew. Chem., Int. Ed. Engl.* **1988**, *27*, 89.
(3) Stiegman, A. E.; Miskowski, W. M.; Perry, J. W.; Coulter, D. R. *J. Am. Chem. Soc.* **1987**, *109*, 5884. Effenberger, F.; Schlosser, H.; Bäuerle, P.; Maier, S.; Port, H.; Wolf, H. C. *Angew. Chem., Int. Ed. Engl.*, **1988**, *27*, 281. Blanchard-Desce, M.; Ledoux, I.; Lehn, J.-M.; Malthete, J.; Zyss, J. *J. Chem. Soc., Chem. Commun.* **1988**, 736. See also references cited in ref 1.
(4) De Vries, J. J.; Berendsen, H. J. C. *Nature* **1969**, *221*, 1139.
(5) Lindblom, G. *Acta Chem. Scand.* **1972**, *26*, 1745.
(6) Johansson, L. B.-Å; Lindblom, G.; Wieslander, Å.; Arvidson, G. *FEBS Lett.* **1981**, *128*, 97.

0022-3654/89/2093-6751$01.50/0